Research Paper

Deletion of Calhm2 alleviates MPTP-induced Parkinson's disease pathology by inhibiting EFHD2-STAT3 signaling in microglia

Xuena Bo[1#], Fei Xie[2,3#], Jingdan Zhang[1], Runze Gu[1], Xiaoheng Li[2], Shuoshuo Li[2], Zengqiang Yuan[2✉], and Jinbo Cheng[1,2✉]

1. Center on Translational Neuroscience, College of Life & Environmental Science, Minzu University of China, Beijing, 100081, China
2. The Brain Science Center, Beijing Institute of Basic Medical Sciences, Beijing, 100850, China
3. School of Basic Medical Sciences, Anhui Medical University, Hefei, 230032, China

#Co-first authors

✉ Corresponding authors: Jinbo Cheng, PhD. Center on Translational Neuroscience, College of Life & Environmental Science, Minzu University of China, Beijing, 100081, China. E-mail: cheng_jinbo@126.com. Zengqiang Yuan, PhD. The Brain Science Center, Beijing Institute of Basic Medical Sciences, Beijing, 100850, China. E-mail: zqyuan@bmi.ac.cn, or zyuan620@yahoo.com.

Abstract

Background: Neuroinflammation is involved in the development of Parkinson's disease (PD). Calhm2 plays an important role in the development of microglial inflammation, but whether Calhm2 is involved in PD and its regulatory mechanisms are unclear.

Methods: To study the role of Calhm2 in the development of PD, we utilized conventional Calhm2 knockout mice, microglial Calhm2 knockout mice and neuronal Calhm2 knockout mice, and established the MPTP-induced PD mice model. Moreover, a series of methods including behavioral test, immunohistochemistry, immunofluorescence, real-time polymerase chain reaction, western blot, mass spectrometry analysis and co-immunoprecipitation were utilized to study the regulatory mechanisms.

Results: We found that both conventional Calhm2 knockout and microglial Calhm2 knockout significantly reduced dopaminergic neuronal loss, and decreased microglial numbers, thereby improving locomotor performance in PD model mice. Mechanistically, we found that Calhm2 interacted with EFhd2 and regulated downstream STAT3 signaling in microglia. Knockdown of Calhm2 or EFhd2 both inhibited downstream STAT3 signaling and inflammatory cytokine levels in microglia.

Conclusion: We demonstrate the important role of Calhm2 in microglial activation and the pathology of PD, thus providing a potential therapeutic target for microglia-mediated neuroinflammation-related diseases.

Keywords: Microglia; Calhm2; Parkinson's disease; Neuroinflammation; Pathology

Introduction

Parkinson's disease (PD) is the second most common age-related neurodegenerative disease, and has been described as a movement disorder [1]. Typical motor features of the disease include bradykinesia, limb stiffness, and tremor. The main pathological features are the progressive loss of dopaminergic (DA) neurons in the substantia nigra (SNc) and the formation of Lewy bodies due to the aggregation of alpha-synuclein [2, 3]. A community-based study in China showed a PD prevalence of 1.37% in people aged > 60 years [4]. The total number of people with PD in China is estimate to be as high as 3.62 million, posing a major challenge in a rapidly aging population [4]. Risk factors in the development of Parkinson's disease include age, genetics, environment, immune status, and sex [5-7]. The

discovery of family mutations that cause PD, such as alpha-synuclein, parkin, PINK1, DJ-1, LRRK2 and ATP13A2 genes, has led to a better understanding of PD [8, 9]. However, the majority (95%) of PD cases are disseminated and are thought to result from a complex interaction between genetic susceptibility and environmental factors [10]. Recent studies suggest that inflammation acts as a bridge between the two and is involved in the development of PD [10, 11].

In 1988, McGeer et al. detected the presence of large numbers of HLA-DR-positive reactive microglia in the SNc of PD patients, which was one of the first pieces of evidence linking neuroinflammation to the pathogenesis of PD [12]. Microglia—resident macrophages in the brain—account for 5–10% of all human brain cells and act as immune monitors of cellular surroundings [13]. Normally, alpha-synuclein aggregates are released from neurons via extracellular secretion, and extracellular alpha-synuclein can diffuse into microglia via intercellular transfer or non-cell-autonomous means [14, 15]. Microglia are unusually sensitive to cell-damage signals generated by dysfunctional neurons. These signals cause them to change from a resting state under healthy conditions to an activated state. Activated microglia exhibit two types of polarization: in the pro-inflammatory stage, microglia secrete large amounts of pro-inflammatory and chemokines, and in the anti-inflammatory stage, they exhibit increased phagocytosis and secrete anti-inflammatory cytokines that play an important role in neuroprotection and tissue repair [16]. Alpha-synuclein disrupts the dynamic balance of microglial polarization by inhibiting microglial autophagy, accompanied by accelerated expression of pro-inflammatory cytokines [17]. This causes irreversible damage to dopamine neurons, which in turn activates microglia, creating a vicious cycle within the SNc of the brain.

Calcium ions are important secondary messengers for cellular function and are stored in the endoplasmic reticulum and mitochondria. Dysregulation of calcium homeostasis is a key feature of PD pathogenesis [18]. In models of PD induced by mutations in the genetic factor GBA1, mutant neurons exhibit dysregulation of calcium homeostasis and increased vulnerability to stress responses, including elevated cytoplasmic calcium levels [19]. PINK1 deficiency causes mitochondrial accumulation of calcium, resulting in mitochondrial calcium overload [20]. L-Ornithine L-Aspartate was found to slow the progression of PD by regulating intra-mitochondrial calcium homeostasis and restoring mitochondrial function in a PD model [21]. Additionally, Rifampicin has been found to reduce neuroinflammation by reducing mitochondrial dysfunction due to impaired calcium homeostasis in PD [22]. The Calcium Homeostasis Modulator (CALHM) family consists of Calhm1 to Calhm6. Calhm1 is the most intensively studied member of this group, and the Calhm1 P86L single nucleotide polymorphism has also been suggested as a risk factor for Alzheimer's disease (AD) [23]. Our previous study found that Calhm2 expression was increased in AD model mice, and that knockout of Calhm2 improved Aβ plaque deposition, reduced neuroinflammation, and improved cognitive impairment in AD model mice. Further studies revealed that microglia-specific knockout of Calhm2 also improved pathological manifestations in AD mice, and both *in vivo* and *in vitro* experiments demonstrated that inhibition of Calhm2 significantly inhibited microglial activation [24]. Calhm2 plays an important role in the development of microglial inflammation, but whether Calhm2 is involved in PD and its regulatory mechanisms are unclear.

In the present study, we found that Calhm2 plays an important role in the 1-Methyl-4-phenyl-1,2,3,6-tetrahydropyridine (MPTP)-induced mouse model of PD. Either conventional knockout of Calhm2 or microglial conditional knockout of Calhm2 rescued the MPTP-induced loss of tyrosine hydroxylase (TH)-positive neurons and inhibited neuroinflammation, thereby improving motor deficits in PD model mice.

Results

Conventional knockout of Calhm2 improves locomotor performance, and reduces DA neuronal loss and microglia numbers

We previously reported that Calhm2 regulated microglial activation-mediated neuroinflammation and played an important role in the pathology of Alzheimer's disease [24]. However, the mechanism by which Calhm2 regulates microglial activation and whether Calhm2 is involved in other neuro-inflammation-related diseases was unclear. In this study, we investigated the role of Calhm2 in MPTP-induced PD and its underlying mechanisms. To that end, Calhm2 knockout mice (Calhm2 KO) and Calhm2 wide-type mice (Calhm2 WT) were used to generate MPTP-induced PD mice model (**Figure S1A**). The mice were subjected to three days of rotarod training, followed by MPTP injection (four intraperitoneal injections at 2 h intervals of 20 mg/kg each in one day), and behavioral testing after 3 and 7 days of MPTP treatment (**Figure 1A**). The results of the first rotarod test showed that after 3 days of MPTP treatment, mice had a significantly lower latency on the cylinder than mice injected with saline, indicating

that MPTP induced PD symptoms, resulting in impaired locomotion in mice. Interestingly, knockout of Calhm2 was found to rescue this phenotype. Consistently, the results of the second rotarod test showed that after 7 days of MPTP treatment, Calhm2 KO mice showed significant enhancement in locomotor performance compared to Calhm2 WT mice (**Figure 1B-C**), suggesting that knockout of Calhm2 was beneficial for MPTP treatment-induced PD symptoms in mice.
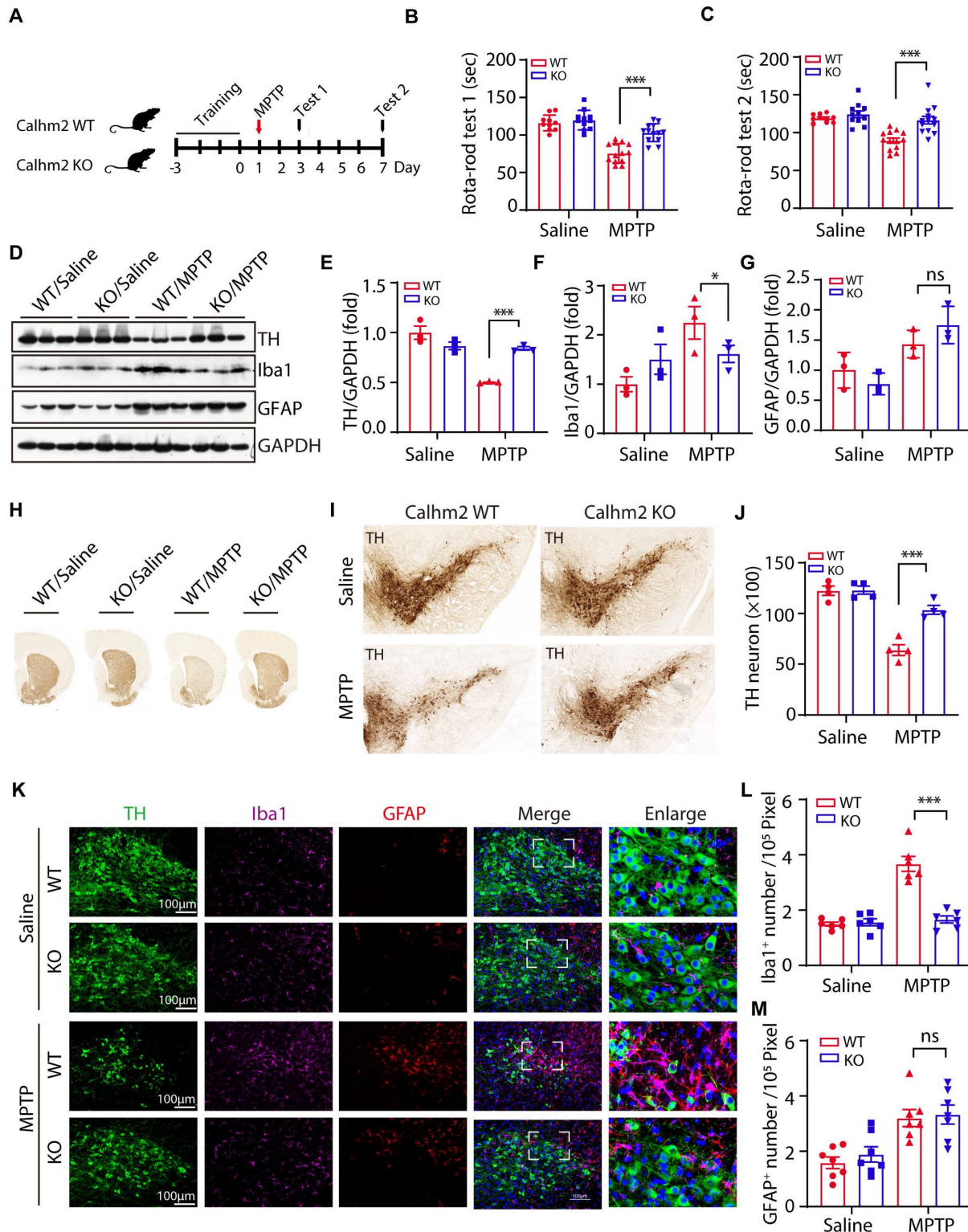

Figure 1. Conventional knockout of Calhm2 improves locomotor performance, reduces DA neuronal loss and microglia numbers. (A) Calhm2 WT and Calhm2 KO mice were treated with saline or MPTP (four intraperitoneal injections of 20 mg/kg, 2 h intervals) after three days of rotarod training. Behavioral tests were performed on the third and seventh day after MPTP injection and striatal tissue was collected on the seventh day. (B and C) Latency of mice on the rotating rod. Data are expressed as mean ± S.E.M. (ANOVA, *$P < 0.05$, **$P < 0.01$, ***$P < 0.001$, n ≥ 10) (D-G) Immunoblotting and statistical analysis of Striatal tissue lysates using antibodies against

Iba1, GFAP, and TH after MPTP treatment (n = 3). (H) Images of immunohistochemically stained sections of mouse striatum treated with anti-TH antibody. (I) Images of immunohistochemically stained sections of TH in the SNc of mice. (J) Statistical analysis of the number of TH-positive neurons in the SNc of mice. Data are expressed as mean ± S.E.M. *$P < 0.05$, **$P < 0.01$, ***$P < 0.001$, n = 4. (K) Co-localization of TH (immunostaining) with Iba1 (immunostaining) and GFAP (immunostaining) positive cells in Calhm2 WT and Calhm2 KO mice. (L, M) Statistical analysis of the number of microglia as well as astrocytes. *$P < 0.05$, **$P < 0.01$, ***$P < 0.001$, (n = 6 slices for 3 mice per group).

Next, we examined whether knockout of Calhm2 altered TH levels in the brain and found that MPTP treatment resulted in a significant reduction in TH protein levels in the striatum compared to the control group, and that Calhm2 knockout significantly restored TH expression levels, suggesting that Calhm2 knockout could restore the loss of TH-positive neurons caused by MPTP treatment. We also examined the expression levels of glial fibrillary acidic protein (GFAP, an astrocyte marker) and ionized calcium-binding adaptor molecule 1 (Iba1, a microglial marker) in the brain. We found that MPTP treatment led to an increase in the expression levels of both GFAP and Iba1, and Calhm2 knockout inhibited Iba1 levels, but not GFAP levels (**Figure 1D-G**). The motor deficits in PD mice were associated with the loss of DA neurons in the SNc; therefore, we further investigated whether Calhm2 knockout could reduce MPTP-induced loss of DA neurons. The number of TH-positive neurons in the SNc was counted using immunohistochemical staining of TH. The results showed that MPTP treatment induced an approximately 50% loss of TH-positive neurons and that Calhm2 knockout significantly restored the loss of TH-positive neurons (**Figure 1H-J**).

Further, we performed immunofluorescence staining of glial cells. We found that under normal conditions, knockout of Calhm2 had no effect on either microglial, or astrocyte numbers. However, MPTP treatment increased both microglial and astrocyte numbers in the mouse brain. Interestingly, knockout of Calhm2 largely reduced the increase in microglial numbers but had no effect on astrocyte numbers in MPTP-treatment conditions (**Figure 1K-M**). Taken together, these results suggest that Calhm2 knockout improves locomotor performance and reduces DA neuronal loss and microglial numbers in PD model mice.

Microglial specific Calhm2 knockout improves locomotor performance and reduces DA neuron loss in PD mice

The above results suggest that Calhm2 is involved in MPTP-induced loss of DA neurons and neuroinflammation. However, the cell type in which Calhm2 operates in the development of PD remains unclear. To investigate this, we crossed a Calhm2 flox/flox mouse strain with Cx3cr1-CreER transgenic mice to obtain a microglial conditional knockout of Calhm2 mice. Mice were gavaged with tamoxifen at 45 days after birth. Microglia were isolated from the

brain one month later to confirm Calhm2 knockout efficiency (**Figure S2A**). After the three-day behavioral training of the rotarod, mice were treated with saline or MPTP separately (four intraperitoneal injections at 2 h intervals of 20 mg/kg each in one day). Behavioral tests of the rotarod were performed 3 and 7 days after MPTP injection, respectively. Additionally, pathological analyses were performed 7 days after MPTP injection (**Figure 2A**). The behavioral results showed that microglial conditional knockout of Calhm2 significantly protected against MPTP-induced motor deficits (**Figure 2B, C**). The loss of nigrostriatal DA neurons was always accompanied by the onset of motor deficits. We then performed immunoblotting experiments and immunohisto-chemical staining, and found that microglial Calhm2-specific knockout prevented the loss of TH protein levels and TH staining signals in the striatum after MPTP treatment (**Figure 2D-H**). Similarly, we stained TH-positive neurons in the SNc using immunohistochemical staining and found that microglia-specific knockout of Calhm2 significantly protected against MPTP-induced loss of TH-positive neurons (**Figure 2I, J**). At the same time, we examined the expression levels of GFAP and IbaI in the brain and found that MPTP injection resulted in elevated expression levels of GFAP (the astrocyte marker), and Iba1 (the microglia marker), and Calhm2 knockout showed a tendency to reduce the elevated Iba1 levels but not the elevated GFAP levels (**Figure 2D, F, G**). Furthermore, we performed immunofluorescence staining of GFAP and Iba1 in the SNc and found that microglial knockout of Calhm2 significantly reduced the increase in microglial numbers, but had no effect on astrocyte numbers under MPTP-treatment conditions (**Figure 2K-M**). Taken together, these results show that microglial conditional knockout of Calhm2 could also rescue MPTP-induced motor defects, DA neuronal loss, and neuroinflammation in PD model mice, suggesting that Calhm2 plays an important role in microglia.

Neuronal Calhm2 knockout has no effect on TH-positive neuron loss and glial activation

To test whether neuronal Calhm2 is involved in the MPTP-induced loss of DA neurons and neuroinflammation, the Calhm2 flox/flox mice were crossed with Camkiiα-iCre transgenic mice to obtain a neuronal conditional knockout of Calhm2 mice. We used the same acute MPTP injection model and performed pathological analysis seven days after

MPTP injection (**Figure 3A**). We found that the level of TH expression in the striatum was significantly reduced after MPTP treatment, but neuronal conditional Calhm2 knockout failed to rescue its level (**Figure 3B, C**). We next examined neuronal loss using immunohistochemical staining of TH-positive neu-

rons in the striatal and SNc regions and found that neuronal specific knockout of Calhm2 had no protective effect against MPTP-induced neuronal cell loss compared to that of the Calhm2 WT group mice (**Figure 3D-F**).
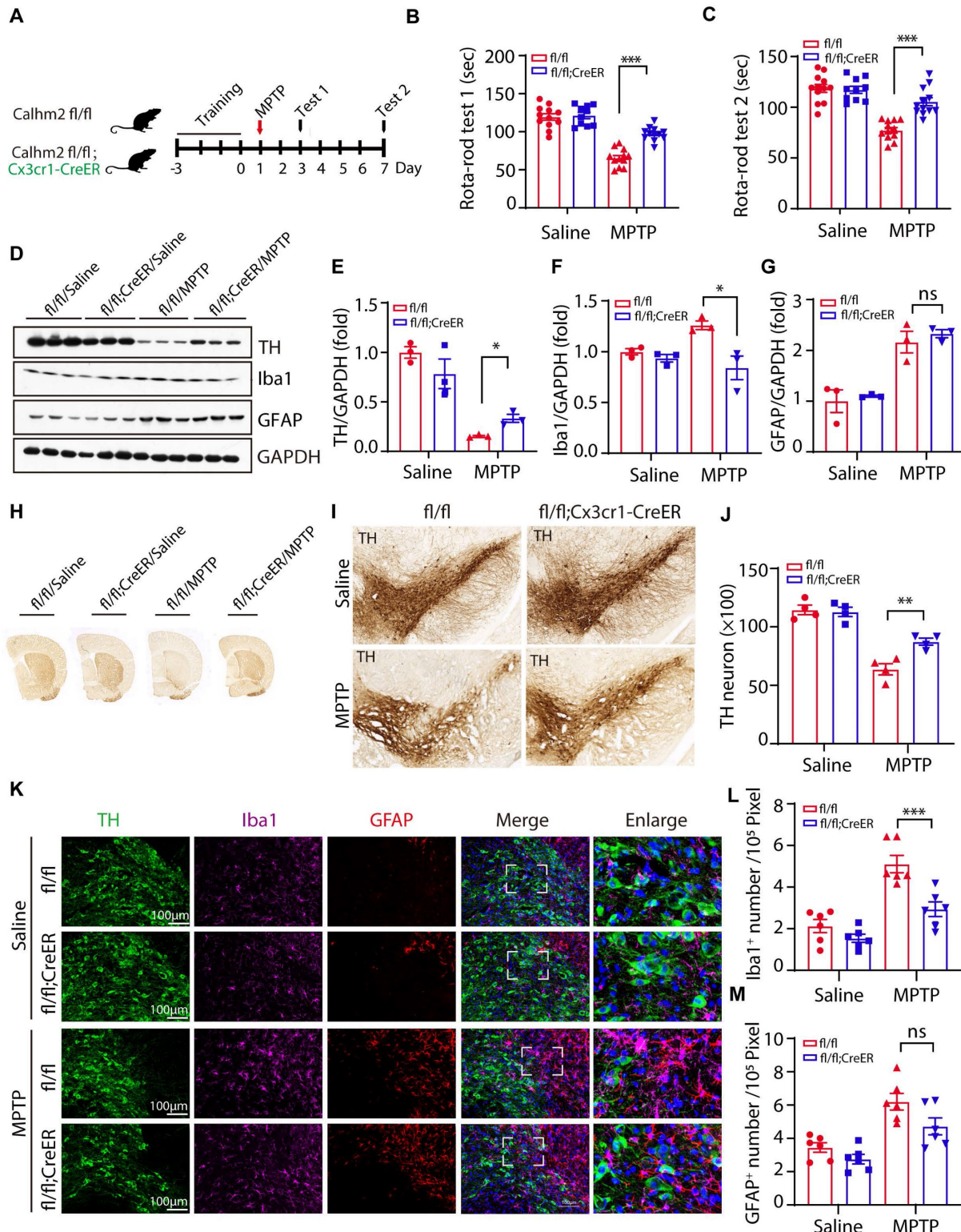

Figure 2. Microglial specific Calhm2 knockout improves locomotor performance and reduces DA neuron loss in PD mice. (A) Experimental flow diagram: 45-day-old Calhm2 flox/flox and Calhm2 flox/flox; Cx3cr1-CreER mice were administered a total dose of 20 mg of intragastric tamoxifen on three consecutive days. Mice were

treated with saline or MPTP (four intraperitoneal injections of 20 mg/kg at 2 h intervals) after three days of rotarod training. Behavioral tests were performed on the third and seventh day after MPTP injection and striatal tissue was collected on the seventh day. (B, C) Latency of mice on the rotating rod. Data are expressed as mean ± S.E.M. (ANOVA, *$P < 0.05$, **$P < 0.01$, ***$P < 0.001$, $n \geq 10$). (D-G) Immunoblotting and statistical analysis of Striatal tissue lysates using antibodies against Iba1, GFAP, and TH after MPTP treatment ($n = 3$). (H) Images of immunohistochemically stained sections of mouse striatum treated with anti-TH antibody. (I) Images of immunohistochemically stained sections of TH in the SNc of mice. (J) Statistical analysis of the number of TH-positive neurons in the SNc of mice. Data are expressed as mean ± S.E.M. *$P < 0.05$, **$P < 0.01$, ***$P < 0.001$, $n = 4$. (K) Co-localization of TH (immunostaining) with Iba1 (immunostaining) and GFAP (immunostaining) positive cells in Calhm2 flox/flox versus Calhm2 flox/flox;Cx3cr1-CreER mice. (L, M) Statistical analysis of the number of microglia as well as astrocytes. *$P < 0.05$, **$P < 0.01$, ***$P < 0.001$, ($n = 6$ slices for 3 mice per group).
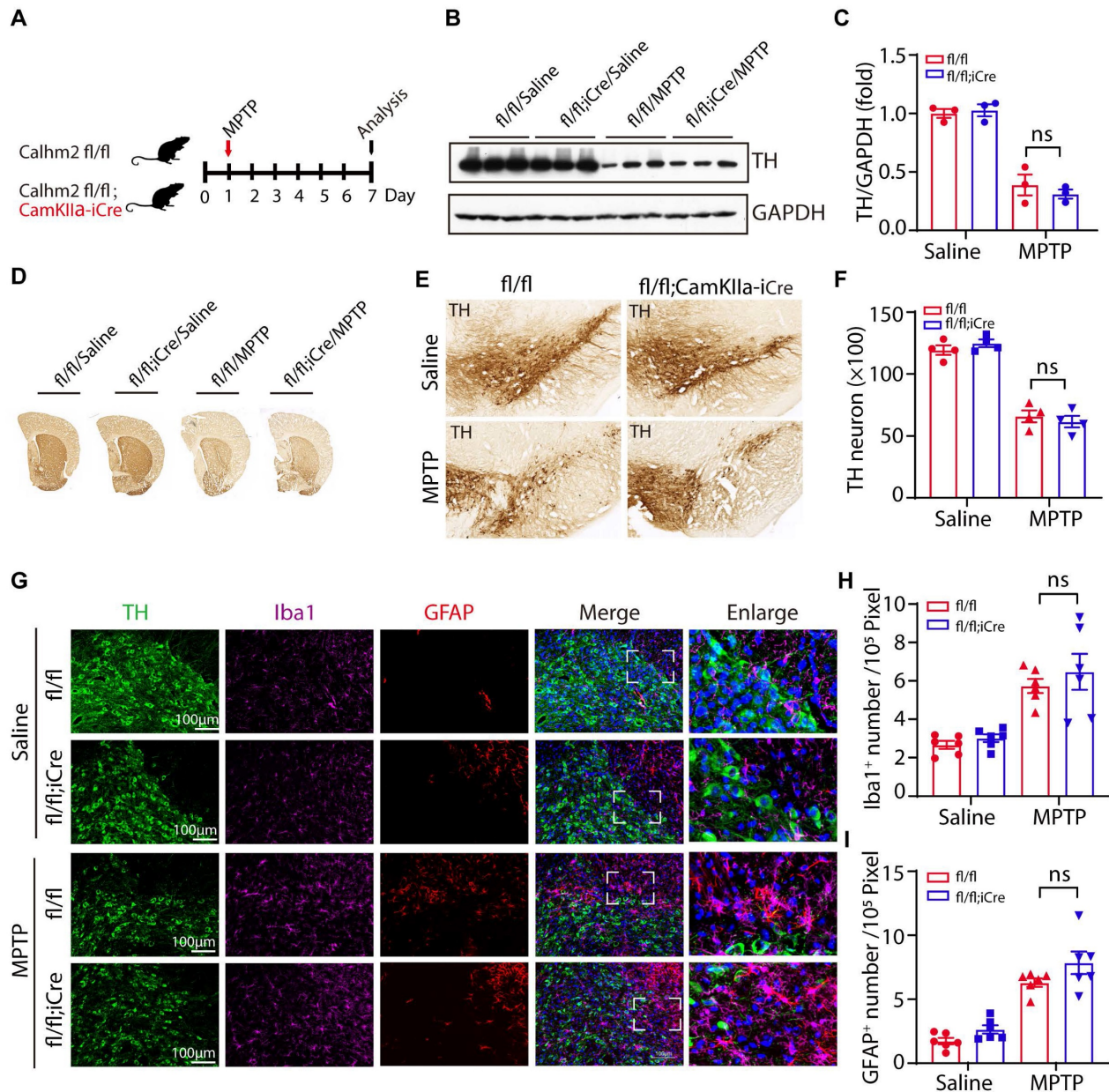

Figure 3. Neuronal Calhm2 knockout has no effect on TH-positive neuron loss and glial activation. (A) Experimental flow diagram: Calhm2 flox/flox treated with saline or MPTP vs. Calhm2 flox/flox; CamKIIα-iCre mice (4 intraperitoneal injections of 20 mg/kg at 2 h intervals). Striatal tissue was collected on day 7 after MPTP injection. (B) Immunoblotting of striatal tissue lysates using anti-TH antibody to label DA neurons after MPTP treatment, using anti-GAPDH as a loading control. (C) Statistical analysis of TH expression levels ($n = 3$). (D) Images of immunohistochemically stained sections of mouse striatum treated with anti-TH antibody. (E) Images of immunohistochemically stained sections of TH in the SNc of mice. (F) Statistical analysis of the number of TH-positive neurons in the SNc of mice represented in A. Data are expressed as mean ± S.E.M. *$P < 0.05$, **$P < 0.01$, ***$P < 0.001$, $n = 4$. (G) TH (immunostaining) versus Iba1 (immunostaining) and GFAP (immunostaining) positive cells in Calhm2 flox/flox; CamKIIα-iCre mice. (H, I) Statistical analysis of the number of microglia as well as astrocytes. *$P < 0.05$, **$P < 0.01$, ***$P < 0.001$, ($n = 6$ slices from 3 mice per group).

In addition, we performed immunofluorescence staining and quantification of glial cell numbers in the region of the SNc, and found that neuronal conditional knockout Calhm2 was unable to inhibit either the increase in microglia numbers or astrocyte numbers induced by MPTP treatment (**Figure 3G-I**). Taken together, these results suggest that neuronal Calhm2 knockout has no effect on TH-positive neuron loss and glial activation.

Calhm2 regulates LPS-induced microglial activation *in vitro*

To further investigate the role of Calhm2 in microglia, we isolated Calhm2 WT and Calhm2 KO primary microglia and stimulated them with lipopolysaccharide (LPS) *in vitro*. Quantitative PCR was used to determine the knockout efficiency of Calhm2, and immunoblotting was used to detect the expression of inducible nitric oxide synthase (iNOS). The results showed that Calhm2 was completely deleted in the Calhm2 KO primary microglia (**Figure 4A**). The expression level of iNOS in WT microglia increased significantly after 6 h of LPS stimulation, whereas the expression level of iNOS in Calhm2 KO microglia was significantly downregulated (**Figure 4B**), indicating that Calhm2 might be involved in the regulation of LPS-induced inflammation. To further investigate the effect of Calhm2 on LPS-induced inflammation levels, we constructed Calhm2 overexpressed plasmid and obtained a stable overexpression of Calhm2 bone marrow-derived macrophage cell line (BMDM). We found that Calhm2 overexpression increased the mRNA levels of TNF-α, IL-1β, and IL-6 induced by LPS stimulation (**Figure 4D-F**), suggesting that overexpression of Calhm2 played a role in promoting LPS-induced inflammation.

To further confirm this, we constructed Calhm2 knockdown plasmid and obtained a stable Calhm2 knockdown BV2 cell line. Consistently, we found that the knockdown of Calhm2 significantly decreased the mRNA levels of TNFα, IL-6, and iNOS under LPS stimulation (**Figure 4G-J**). Interestingly, Calhm2 knockdown also significantly decreased the mRNA levels of iNOS, TNFα, and IL-6 under LPS and MPP+ co-stimulation conditions (**Figure 4G-J**), indicating that Calhm2 plays a positive role in the inflammatory response of microglia induced by MPP+ and LPS treatment.

EF-hand domain family member D2 (EFhd2) interacts with Calhm2 in microglia cell line and mouse brain tissue

Next, to investigate the regulatory mechanism of Calhm2 in microglia, we used BV2 overexpressing Calhm2 cell lines and immunoprecipitated Flag-Calhm2 from the cell lysates and performed a mass spectrometry analysis to identify the possible interacting proteins (**Figure 5A**). The results showed that Calhm2 protein bands were enriched only in the overexpression group (**Figure 5B**). Moreover, the mass spectrometry results showed that EFhd2 and actin-related protein 2/3 complex subunit 1 B (Arpc1B) interacted with Calhm2 (**Figure 5C**). To further identify the interacting protein of Calhm2, we constructed an HA-tag at the C-terminus of the Calhm2 gene and obtained HA-Calhm2 transgenetic mice (**Figure 5D**). Genotyping and HA tag expression are verified in **Figure S3A and S3B**.

To investigate the interaction proteins of Calhm2 in mice brain, the brain tissue of Calhm2 WT and Calhm2-HA mice were lysed and immuno-precipitated, and mass spectrometry analysis was performed to identify possible interacting proteins. Consistently, we found that EFhd2 and Arpc1B also interacted with Calhm2 in mice brain tissue. To further validate the interaction between Calhm2 and EFhd2, we transfected HA-tagged Calhm2 and Myc-tagged EFhd2 plasmids into HEK293T cells and performed immunoprecipitation. We found that EFhd2 interacted with Calhm2 in these cells (**Figure 5F**). Interestingly, a slight increase in the interaction between EFhd2 and Calhm2 occurred under LPS stimulation conditions in the cells.

Calhm2 regulates the phosphorylation of EFhd2 and the downstream STAT3 signaling in microglia

To investigate the relationship between Calhm2 and EFhd2 (**Figure 6A**), we used an acute LPS-stimulated cellular model in Calhm2 knockdown BV2 cells and found that knockdown of Calhm2 did not change the protein levels of EFhd2 in microglia (**Figure 6B**). Consistently, we found that either Calhm2 knockout or Calhm2 overexpression both failed to impair the EFhd2 protein levels (**Figure S4A and S4B).** It has been reported that tyrosine phosphorylation of EFhd2 is involved in LPS-induced inflammatory response in macrophages [25]. Therefore, we performed immunoprecipitation experiments and found that the tyrosine phosphorylated EFhd2 levels were lower in Calhm2 knockdown microglia cells under LPS stimulation conditions, suggesting that Calhm2 might regulate tyrosine phosphorylation of EFhd2 in microglia (**Figure 6C**).

As previously reported, EFhd2 regulates LPS-induced inflammatory response in macrophages by modulating downstream STAT3 signaling [26]. To further investigate the role of EFhd2 in LPS-induced inflammatory response and its regulatory mechanism (**Figure 6D**), we examined the downstream phosphorylated STAT3 levels in microglia upon LPS treatment. We found that phosphorylated STAT3 protein levels were largely reduced in Calhm2 knockdown cells upon LPS stimulation (**Figure 6E**). Consistently, we found that intracellular phosphorylated STAT3 levels were significantly reduced in EFhd2 knockdown microglial cells under LPS stimulation (**Figure 6F**). Together, these results suggest that Calhm2 regulates the phosphorylation of EFhd2 and downstream STAT3 signaling in microglia.
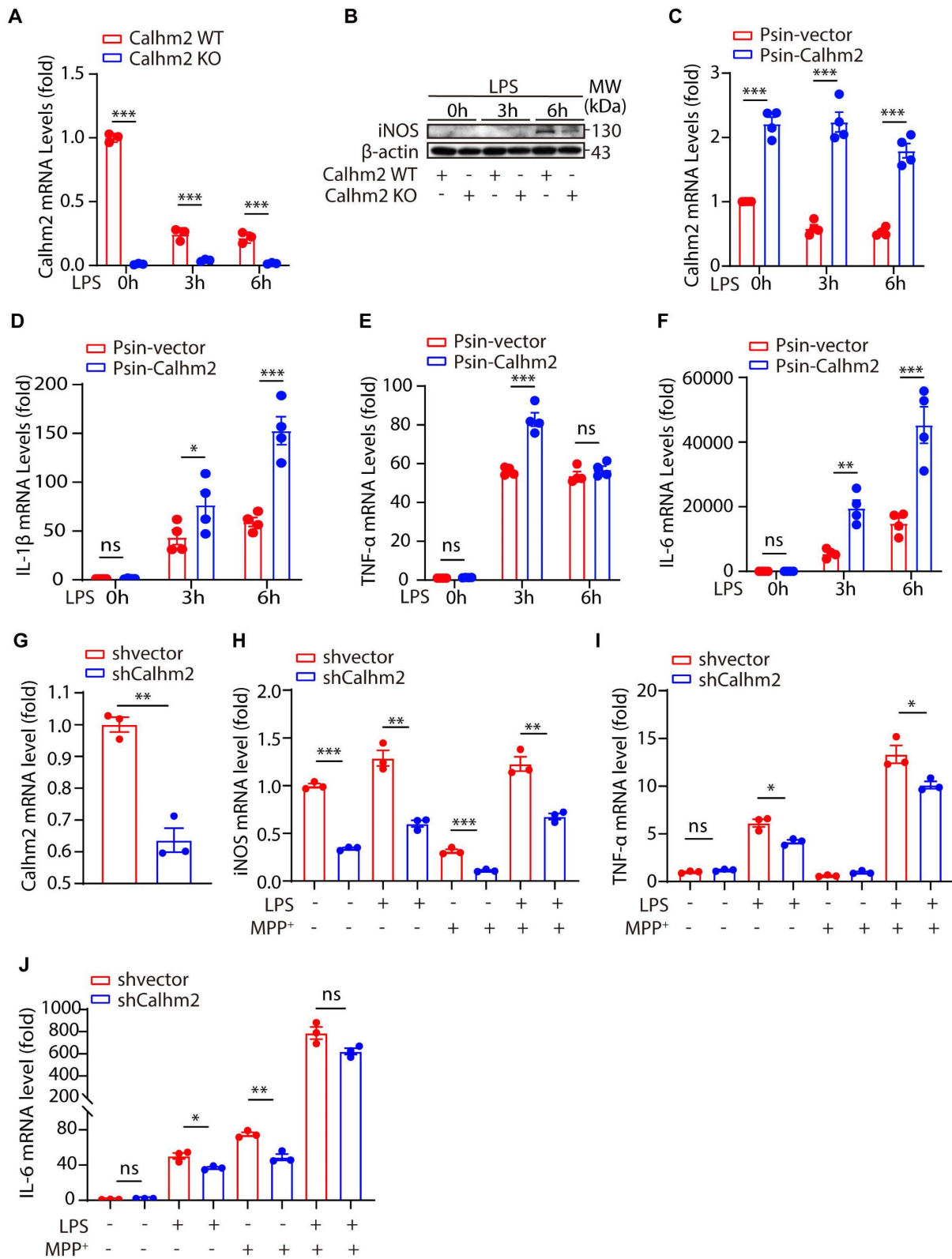
Figure 4. Calhm2 regulates LPS-induced microglial activation *in vitro*. (A) Statistical results of Calhm2 expression in Calhm2 WT and Calhm2 knockout mouse primary microglia stimulated with LPS (1 μg/ml) at different time points. (B) Immunoblotting of control and Calhm2 knockout mouse primary microglia after stimulation with LPS (1 μg/ml) at different time points to compare the expression of iNOS in control and Calhm2 knockout group cells. (C-F) Expression of Calhm2, TNFα, IL-1β and IL-6 in control and overexpressed cells by quantitative PCR after LPS stimulation at different time points in IBMDM normal control cells and overexpressed Calhm2 cells. Statistical results are shown as mean ± S.E.M, * $P < 0.05$, ** $P < 0.01$, *** $P < 0.001$. (G-J) Control and Calhm2 knockdown BV2 cells were stimulated with LPS (0.1 μg/ml) and MPP+ (1 μg/ml) for 12 h. The expression of Calhm2, TNFα, IL-1β and IL-6 was measured by quantitative PCR and the statistical results showed mean ± S.E.M, *$P < 0.05$, **$P < 0.01$, ***$P < 0.001$.
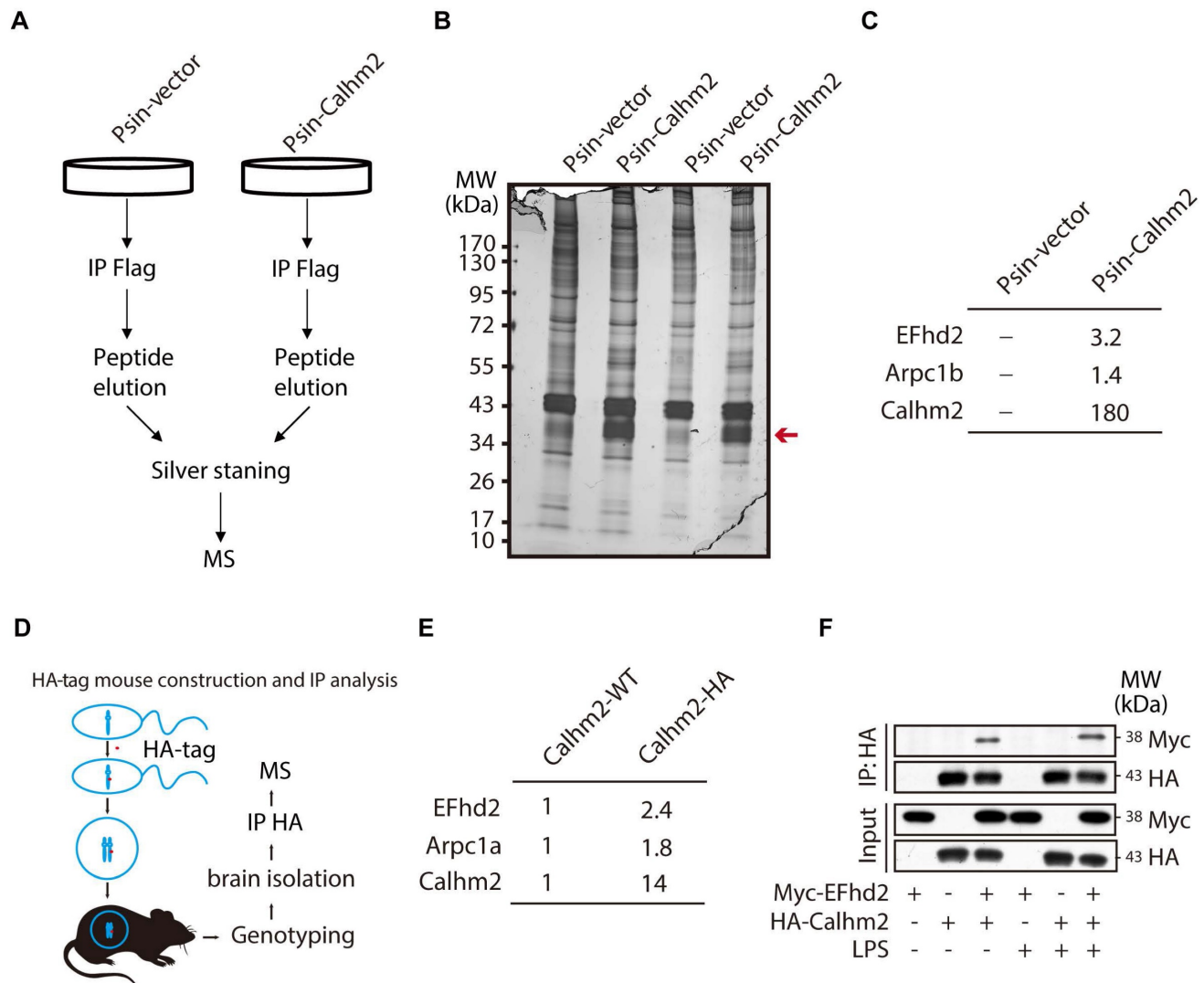
Figure 5. Calhm2 interacts with EFhd2. (A) Flow chart of cells collected, immunoprecipitation of Flag, silver stained, and mass spectrometry analysis in BV2 control cells and overexpressed Calhm2 cells; (B) Silver staining results of immunoprecipitation of Flag samples for proteins. (C) Mass spectrometry results analyzing protein peptide segment differences within control and overexpressed Calhm2 cells. (D) Pattern diagram of Calhm2-HA mouse constructs. (E) Immunoprecipitation using Calhm2 WT with Calhm2 HA mouse brain tissues, and mass spectrometry results analyzing Calhm2 HA interacting proteins. (F) Co-transfection of Myc-EFhd2 and HA-Calhm2 plasmids in HEK293T cells, LPS stimulation for 6 h, and immunoblotting for Myc and HA after immunoprecipitation of HA.

Knockdown of EFhd2 also significantly inhibits LPS-induced inflammation levels in BV2 cells

To investigate the role of EFhd2 in LPS-induced cellular inflammation, we used stable knockdown EFhd2 microglial cell lines and treated them with LPS (**Figure 7A**). We found that the knockdown efficiency of EFhd2 was high in the two stable knockdown cell lines (**Figure 7B**). Moreover, intracellular inflammatory factors such as iNOS, TNFα, and IL-1β were significantly increased upon LPS stimulation, whereas knockdown of EFhd2 significantly suppressed these inflammatory cytokine levels (**Figure 7C-F**). Together, these results suggest that EFhd2 also plays a positive role in LPS-induced microglial inflammation levels.

In summary, we demonstrated that Calhm2 plays an important role in the MPTP-induced PD mouse model. Both conventional and microglial conditional knockout of Calhm2 rescued MPTP-induced TH-positive neuronal loss and inhibited neuroinflammation, thereby improving motor deficits in PD model mice. Mechanistically, we found that Calhm2 interacted with EFhd2 and regulated downstream STAT3 signaling in microglia, presenting a potential therapeutic target for microglia-mediated neuroinflammation-related diseases (**Figure 7G**).

Discussion

Over the past decades, age, genetics, environment, immune status, and sex have been widely discussed as important factors in the development of PD. However, the molecular mechanisms underlying PD pathogenesis are not yet fully understood. Neuroinflammation caused by neuroglia (astrocytes

and microglia) present in the brain is a common feature of PD [27]. In our previous study, we found that defective microglial autophagy accelerates inflammatory vesicle activation in mice, causing PD-like symptoms [28]. Therefore, targeting microglia-mediated neuroinflammation for the treatment of central nervous system disorders is an emerging remedy. In this study, we used conventional Calhm2, neuronal Calhm2, and microglial Calhm2 knockout mice to explore the role of Calhm2 in Parkinson's disease. We found that both conventional and microglial conditional Calhm2 knockout significantly reduced DA neuronal loss and microglial numbers, thereby improving locomotor performance in PD model mice. Thus, our results strongly support the important role of Calhm2 in PD, possibly through the modulation of microglial activation.

Calcium homeostasis in cells was an important factor in the development of neuroinflammation, and dysregulation of Ca^{2+} homeostasis was also frequently observed in models of sporadic and familial PD [29]. More importantly, clinical trials showed that dihydropyridine calcium channel blocker (DiCCB) exposure was associated with a reduced risk of PD incidence, particularly in older patients, and with reduced mortality among patients with PD [30]. Inhibition of TRPM2 by AG490 has been reported to be neuroprotective in a PD Animal Model [31]. Meanwhile, calcium-sensing receptors have been

reported to activate the NLRP3 inflammasome by enhancing intracellular calcium levels and inhibiting cAMP levels [32]. Moreover, blocking calcium channels with Nicardipine significantly inhibited microglial activation *in vitro* [33]. In this study, we found that both knockout of Calhm2 and knockdown of Calhm2 significantly reduced LPS-induced inflammatory cytokine levels, whereas overexpression of Calhm2 significantly increased LPS-induced inflammation, suggesting that Calhm2 plays an important role in microglia-mediated neuroinflammation. This finding is consistent with previous studies showing that reducing intracellular calcium ion concentrations by inhibiting calcium channel proteins contributes to lower levels of neuroinflammation [24]. Our results suggest that targeting Calhm2 could be a possible way to reduce neuroinflammation and thereby improve neurological disease.

Calhm2, a membrane protein, has been shown to mediate the transport of calcium and adenosine triphosphate (ATP), regulating both intra- and extracellular calcium and ATP concentrations [34-36]. Our previous study showed that Calhm2 is abundantly expressed in the central nervous system, and knockout of microglial Calhm2 in AD model mice improved cognitive memory and pathological performance [24]. However, the mechanism through which Calhm2 regulates microglial activation remains unclear. In this study, we found that Calhm2 interacted with EFhd2, a calcium-binding protein that
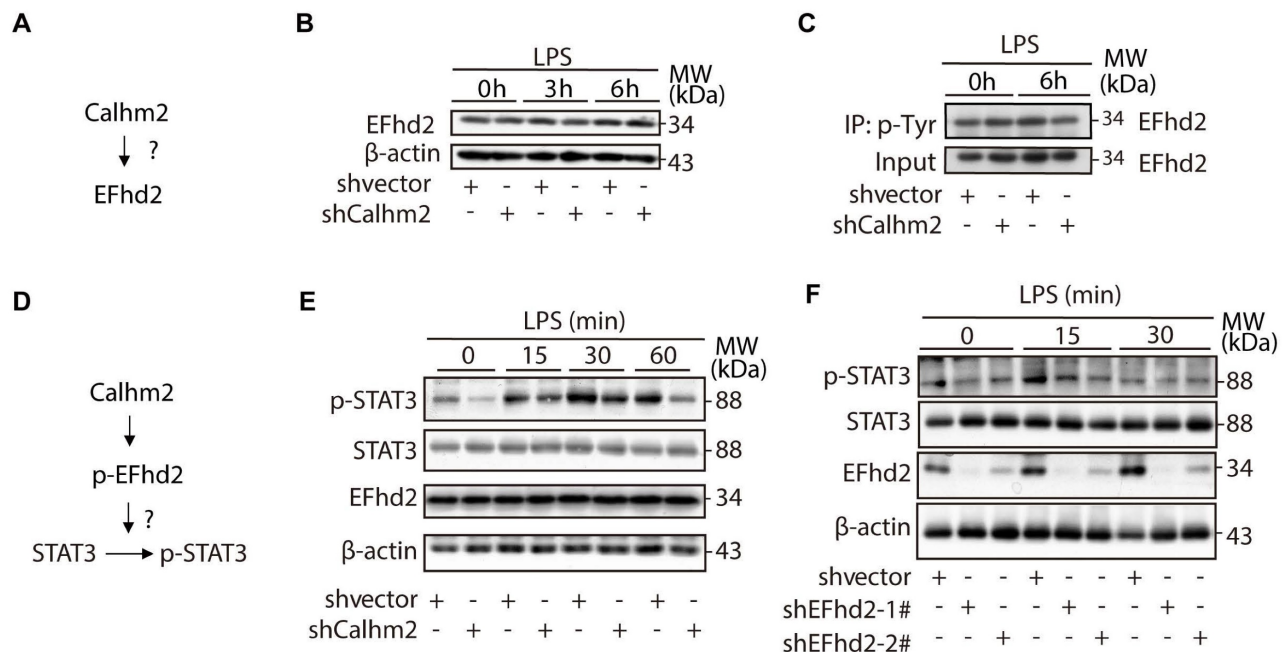

Figure 6. Calhm2 regulates the phosphorylation of EFhd2 and downstream STAT3 signaling in microglia. (A) Diagram of the experimental model. (B) Expression of EFhd2 in control and Calhm2 knockdown cells by immunoblotting after LPS stimulation of BV2 normal control cells and knockdown Calhm2 cells at different time points. (C) Immunoprecipitation of phosphotyrosine and immunoblot detection of EFhd2 in BV2 normal control cells and knockdown Calhm2 cells after LPS stimulation for 6 h, (D) Diagram of the experimental model. (E) Expression of EFhd2, p-STAT3 and STAT3 in control and Calhm2 knockdown cells by immunoblotting after LPS stimulation at different time points. (F) Expression of EFhd2, p-STAT3 and STAT3 in control and EFhd2 knockdown cells by immunoblotting after LPS stimulation at different time points.

possesses two EF chiral structures that bind calcium ion to maintain the normal conformation and the function [37]. A previous study showed that knockdown of EFhd2 significantly reduced LPS-induced inflammation in macrophages; however, the role of EFhd2 in microglia remains unclear [25]. In this study, we found that EFhd2 knockdown in microglia also significantly suppressed LPS-induced inflammation, which was achieved by regulating downstream STAT3 signaling. Overactivation of STAT3 has been reported to lead to the secretion of pro-inflammatory factors in microglia and promote neuronal loss [38], suggesting that tight regulation of STAT3 function is critical to the pathology of PD. We also found that knockdown of either Calhm2 or EFhd2 significantly reduced LPS-induced STAT3 activation, suggesting that Calhm2 may regulate STAT3 signaling through interaction with EFhd2 in microglia.
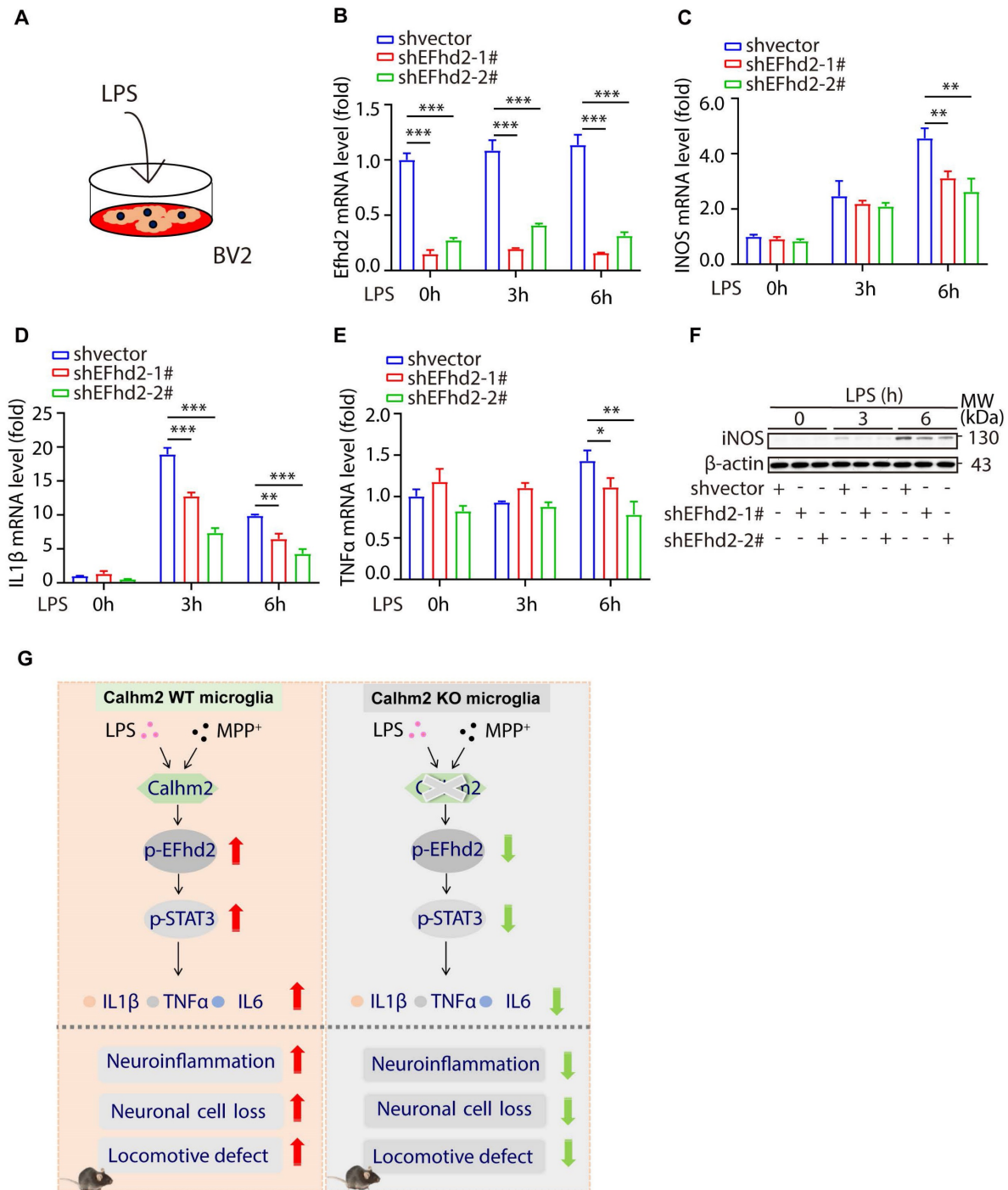

Figure 7. Knockdown of EFhd2 significantly inhibits LPS-induced inflammation levels in BV2 cells. (A) Diagram of the experimental model. (B-E) Quantitative PCR of expression of EFhd2, iNOS, TNFα and IL-1β in control and knockdown EFhd2 cells after LPS stimulation at different time points; statistical results are shown as mean ± S.E.M, *$P < 0.05$, **$P < 0.01$, ***$P < 0.001$. (F) Expression of iNOS and EFhd2 in control and knockdown EFhd2 cells was measured by immunoblotting after LPS stimulation at different time points, using anti-β-actin as a loading control. (G) The working model of microglial Calhm2 in PD mouse model.

In conclusion, we demonstrated that microglial Calhm2 is involved in microglia-mediated neuroinflammation and the pathogenesis of PD by modulating the EFhd2-STAT3 pathway in microglia, which provides potential therapeutic targets for microglia-mediated neuroinflammation-related diseases.

Materials and methods

Mice

The Calhm2 mice used in this experiment have been described in our previous study [24]. Mice were housed in an SPF-rated animal house, provided with a constant temperature of 20–23 °C, maintained on a 12-h diurnal cycle, and provided with an ad libitum diet and water. All animal experiments were approved by the Institutional Animal Care and Use Committee of Beijing Institute of Basic Medical Sciences.

Tamoxifen (Sigma-Aldrich, catalogue no. T5648) was dissolved in corn oil (Sigma-Aldrich, catalogue no. C8267). Intragastric tamoxifen (20 mg) was administered to the mice on three consecutive days.

Calhm2-HA transgenetic mice

An HA-tag was added to the C-terminus of the mouse Calhm2 gene. Calhm2-C-WT and Calhm2-C-HA PCR primers were used to distinguish wild-type, heterozygous, and homozygous. Calhm2-WT: F: GCTCACTGCTTAAGAGCCTG; R: TCCCAGTGGGTTGTCAACAG; Calhm2-HA: F: GTGTTCCTGACCAAGTGCCT; R: ATCCGGCACAT CATACGGAT (95 °C 7 min; 95 °C 15 s, 60 °C 20 s, 72 °C 30 s, 35 Cycle; 72 °C 10 min; 4 °C).

Rotarod test

An accelerated rotating rod (Panlab, LE8200; Energia, Cornella, Spain) was used to evaluate motor impairment in mice. For training, mice were placed on the rod at a constant speed of 10 rpm, 3 times a day (1 h interval) for 3 days prior to the test. During the test, the rod was accelerated from 4 rpm to 40 rpm for 300 s. The time spent on the rod was recorded for each mouse, each mouse was tested three times at 1 h intervals and the average of the three tests was taken as the mean latency for each mouse.

Cell culture and stable cell line

DMEM basic medium and penicillin-Streptomycin were purchased from Life technologies corporation and Fetal Bovine Serum (FBS) was purchased from Biological Industries. Cells were passaged when the growth density of adherent cells reached 70–90%. We add 1 ml of 0.05% trypsin, in a semi-suspension state and used 1 ml of culture solution (10% FBS and, 1% penicillin-Streptomycin) to terminate the digestion, we then centrifuged at 800 rmp for 5 min and aspirated off the supernatant. 1/3 of the cells was incubated at 37 °C in an incubator with 5% CO_2 cells.

Isolation of microglia

Microglia were isolated and purified as described in previous studies [24]. Briefly, the mice were anesthetized by intraperitoneal injection of sodium pentobarbital (70 mg/kg, dissolved in saline). The whole brain tissue was isolated, scalpel cut into small pieces, suspended in Dounce buffer [1.5 mM Hepes and 0.5% glucose in hanks' balanced salt solution (HBSS) buffer] and gently homogenized using a homogenizer. After blowing the cells with phosphate-buffered saline buffered salt solution [PBS; NaCl (8 g/l), KCl (0.2 g/l), Na2HPO4 (1.44 g/l), and KH2PO4 (0.24 g/l)], they were passed through a 70 µm filter; myelin proteins were then removed by differential centrifugation with cell separator Percoll to obtain a single cell suspension; erythrocyte lysate was used to remove hemoglobin; microglia were purified using Miltenyi's CD11b magnetic beads (Miltenyi Biotec, 130-093-634).

Immunohistochemistry and Immunofluorescence

All procedures were performed as described in previous studies [28]. Briefly, mice were perfused with saline and their brains were fixed with 4% paraformaldehyde (w/v). The fixed mouse brains were cryoprotected in 30% sucrose. Coronal sections were cut to a thickness of 40 µm and stained with GFAP (1:1000; Sigma-Aldrich, catalogue no. G3893), Iba1 (1:500; NOVUS; NB100-1028), TH (1:500; Pel-Freez, catalogue no. P40101-150). Coronal sections were incubated with rabbit polyclonal anti-TH (1:500, Pel Freez Biologicals, P40101, Rogers, AR, USA) followed by a horseradish peroxidase (HRP) reaction using the ABC method (VECTASTAIN ABC Kit, Rabbit, IgG, ZF0328). Signal amplification was carried out at a ratio of 1:100 between A and B liquids. The reaction was carried out at room temperature for 30 min, visualized using a DAB kit (1:20, ORIGENE, ZLI-9019), and scanned using a digital pathology section scanning analysis system. Immunohistochemistry (IHC) quantification was performed using Image-Pro Plus software (Media Cybernetics Inc.). To quantify the Iba1 or GFAP IHC levels, we calculated all intact cells in the same pixel region in the indicated brain regions.

Immunoprecipitation and Immunoblot Analysis

Immunoprecipitation and immunoblot analyses

were performed as described in previous study [24]. Briefly, tissues for co-immunoprecipitation were lysed in a buffer containing 50 mM Nacl (pH 7.4), 1 mM EDTA, 1 mM EGTA, and 0.05% Triton-100. Prior to immunoprecipitation, the tissue was lysed to remove the supernatant and pre-incubated with protein G agarose beads for 1 h at 4 °C. After removal of the beads by centrifugation, the lysates were incubated with the appropriate antibody in the presence of 25 µl protein G agarose beads for at least 3 h at 4 °C. After three washes, protein expression was detected by western blotting of cell lysates or immunoprecipitates using the appropriate antibodies; that is, the proteins were separated on a 10% polyacrylamide gel and transferred to NC membranes. The membranes were incubated in Tris-buffered saline containing 5% milk and Tween-20 for 1 h, followed by incubation with primary antibody overnight at 4 °C. After incubation with goat anti-mouse or goat anti-rabbit HRP-coupled secondary antibodies (GE Healthcare) for 1 h, the indicated protein was detected using an enhanced chemiluminescence western blotting system (Amersham Biosciences).

Quantitative RT-PCR

Total RNA was extracted from the brain tissue or cells using TRIzol reagent (Invitrogen, catalogue no. 15596018). One microgram of RNA was used as a template for the one-step first-strand cDNA synthesis kit (AT341). PCR amplification was performed using a 2 × SYBR Green PCR master mix (TransGen Biotech, catalogue number: AQ131) and an Agilent Mx3005P RT-PCR system, and gene expression was detected. The primers used for the analysis are listed in **Supplementary Table 1**. The mRNA levels of the tested genes were normalized to that of β-actin.

Statistical Analysis

Image Pro and GraphPad software were used for data statistics and analysis. Unpaired Students and two-tailed t test, and two-way ANOVA were used to determine significance between the data. In all experiments, $P < 0.05$ was considered a statistically significant difference.

Abbreviations

AD: Alzheimer's disease; ATP: adenosine triphosphate; Arpc1B: actin-related protein 2/3 complex subunit 1 B; BMDM: bone marrow-derived macrophage; CALHM: calcium homeostasis modulator; Calhm2 KO: Calhm2 knockout; Calhm2 WT: Calhm2 wide-type; DA: dopaminergic; EFhd2: EF-hand domain family member D2; FPS: Fetal Bovine Serum; GFAP: glial fibrillary acidic protein; HRP: horseradish peroxidase; Iba1: ionized calcium-binding adaptor molecule 1; IHC: immunohisto-chemistry; iNOS: inducible nitric oxide synthase; LPS: lipopolysaccharide; MPTP: 1-Methyl-4-phenyl-1,2,3,6-tetrahydropyridine; PD: Parkinson's disease; SNc: substantia nigra; TH: tyrosine hydroxylase.

Supplementary Material

Supplementary figures and table.
https://www.thno.org/v13p1809s1.pdf

Author contributions

Xuena Bo designed and performed experiments, analyzed data, and wrote the paper. Fei Xie performed some experiments and analyzed data. Jingdan Zhang, Runze Gu, Xiaoheng Li and Shuoshuo Li analyzed data. Zengqiang Yuan and Jinbo Cheng supervised this research, analyzed data, and wrote the paper.

Competing Interests

The authors have declared that no competing interest exists.

References

[1] de Lau LM, Breteler MM. Epidemiology of Parkinson's disease. Lancet Neurol 2006;5:525-35.
[2] Moore DJ, West AB, Dawson VL, Dawson TM. Molecular pathophysiology of Parkinson's disease. Annu Rev Neurosci 2005;28:57-87.
[3] Pistacchi M, Gioulis M, Sanson F, De Giovannini E, Filippi G, Rossetto F, et al. Gait analysis and clinical correlations in early Parkinson's disease. Funct Neurol 2017;32:28-34.
[4] Qi S, Yin P, Wang L, Qu M, Kan GL, Zhang H, et al. Prevalence of Parkinson's Disease: A Community-Based Study in China. Mov Disord 2021;36:2940-4.
[5] Pajares M, A IR, Manda G, Bosca L, Cuadrado A. Inflammation in Parkinson's Disease: Mechanisms and Therapeutic Implications. Cells 2020;9.
[6] Cerri S, Mus L, Blandini F. Parkinson's Disease in Women and Men: What's the Difference? J Parkinsons Dis 2019;9:501-15.
[7] Tansey MG, Wallings RL, Houser MC, Herrick MK, Keating CE, Joers V. Inflammation and immune dysfunction in Parkinson disease. Nat Rev Immunol 2022;22:657-73.
[8] Banerjee R, Starkov AA, Beal MF, Thomas B. Mitochondrial dysfunction in the limelight of Parkinson's disease pathogenesis. Biochim Biophys Acta 2009;1792:651-63.
[9] Crosiers D, Theuns J, Cras P, Van Broeckhoven C. Parkinson disease: insights in clinical, genetic and pathological features of monogenic disease subtypes. J Chem Neuroanat 2011;42:131-41.
[10] Subramaniam SR, Chesselet MF. Mitochondrial dysfunction and oxidative stress in Parkinson's disease. Prog Neurobiol 2013;106-107:17-32.
[11] La Vitola P, Balducci C, Baroni M, Artioli L, Santamaria G, Castiglioni M, et al. Peripheral inflammation exacerbates alpha-synuclein toxicity and neuropathology in Parkinson's models. Neuropathol Appl Neurobiol 2021;47:43-60.
[12] McGeer PL, Itagaki S, Boyes BE, McGeer EG. Reactive microglia are positive for HLA-DR in the substantia nigra of Parkinson's and Alzheimer's disease brains. Neurology 1988;38:1285-91.

[13] Colonna M, Butovsky O. Microglia Function in the Central Nervous System During Health and Neurodegeneration. Annu Rev Immunol 2017;35:441-68.

[14] Desplats P, Lee HJ, Bae EJ, Patrick C, Rockenstein E, Crews L, et al. Inclusion formation and neuronal cell death through neuron-to-neuron transmission of alpha-synuclein. Proceedings of the National Academy of Sciences of the United States of America 2009;106:13010-5.

[15] Kim C, Ho DH, Suk JE, You S, Michael S, Kang J, et al. Neuron-released oligomeric alpha-synuclein is an endogenous agonist of TLR2 for paracrine activation of microglia. Nature communications 2013;4:1562.

[16] Tang Y, Le W. Differential Roles of M1 and M2 Microglia in Neurodegenerative Diseases. Mol Neurobiol 2016;53:1181-94.

[17] Tu HY, Yuan BS, Hou XO, Zhang XJ, Pei CS, Ma YT, et al. alpha-synuclein suppresses microglial autophagy and promotes neurodegeneration in a mouse model of Parkinson's disease. Aging Cell 2021;20:e13522.

[18] Virdi GS, Choi ML, Evans JR, Yao Z, Athauda D, Strohbuecker S, et al. Protein aggregation and calcium dysregulation are hallmarks of familial Parkinson's disease in midbrain dopaminergic neurons. NPJ Parkinsons Dis 2022;8:162.

[19] Schondorf DC, Aureli M, McAllister FE, Hindley CJ, Mayer F, Schmid B, et al. iPSC-derived neurons from GBA1-associated Parkinson's disease patients show autophagic defects and impaired calcium homeostasis. Nat Commun 2014;5:4028.

[20] Gandhi S, Wood-Kaczmar A, Yao Z, Plun-Favreau H, Deas E, Klupsch K, et al. PINK1-associated Parkinson's disease is caused by neuronal vulnerability to calcium-induced cell death. Mol Cell 2009;33:627-38.

[21] Sisalli MJ, Della Notte S, Secondo A, Ventra C, Annunziato L, Scorziello A. L-Ornithine L-Aspartate Restores Mitochondrial Function and Modulates Intracellular Calcium Homeostasis in Parkinson's Disease Models. Cells 2022;11.

[22] Yurtsever I, Ustundag UV, Unal I, Ates PS, Emekli-Alturfan E. Rifampicin decreases neuroinflammation to maintain mitochondrial function and calcium homeostasis in rotenone-treated zebrafish. Drug Chem Toxicol 2022;45:1544-51.

[23] Dreses-Werringloer U, Lambert JC, Vingtdeux V, Zhao H, Vais H, Siebert A, et al. A polymorphism in CALHM1 influences Ca2+ homeostasis, Abeta levels, and Alzheimer's disease risk. Cell 2008;133:1149-61.

[24] Cheng J, Dong Y, Ma J, Pan R, Liao Y, Kong X, et al. Microglial Calhm2 regulates neuroinflammation and contributes to Alzheimer's disease pathology. Science advances 2021;7.

[25] Tu Y, Zhang L, Tong L, Wang Y, Zhang S, Wang R, et al. EFhd2/swiprosin-1 regulates LPS-induced macrophage recruitment via enhancing actin polymerization and cell migration. Int Immunopharmacol 2018;55:263-71.

[26] Zhang S, Tu Y, Sun YM, Li Y, Wang RM, Cao Y, et al. Swiprosin-1 deficiency impairs macrophage immune response of septic mice. JCI Insight 2018;3.

[27] Kwon HS, Koh SH. Neuroinflammation in neurodegenerative disorders: the roles of microglia and astrocytes. Transl Neurodegener 2020;9:42.

[28] Cheng J, Liao Y, Dong Y, Hu H, Yang N, Kong X, et al. Microglial autophagy defect causes parkinson disease-like symptoms by accelerating inflammasome activation in mice. Autophagy 2020;16:2193-205.

[29] Post MR, Lieberman OJ, Mosharov EV. Can Interactions Between alpha-Synuclein, Dopamine and Calcium Explain Selective Neurodegeneration in Parkinson's Disease? Front Neurosci 2018;12:161.

[30] Pasternak B, Svanstrom H, Nielsen NM, Fugger L, Melbye M, Hviid A. Use of calcium channel blockers and Parkinson's disease. American journal of epidemiology 2012;175:627-35.

[31] Ferreira AFF, Singulani MP, Ulrich H, Feng ZP, Sun HS, Britto LR. Inhibition of TRPM2 by AG490 Is Neuroprotective in a Parkinson's Disease Animal Model. Molecular neurobiology 2022;59:1543-59.

[32] Lee GS, Subramanian N, Kim AI, Aksentijevich I, Goldbach-Mansky R, Sacks DB, et al. The calcium-sensing receptor regulates the NLRP3 inflammasome through Ca2+ and cAMP. Nature 2012;492:123-7.

[33] Huang BR, Chang PC, Yeh WL, Lee CH, Tsai CF, Lin C, et al. Anti-neuroinflammatory effects of the calcium channel blocker nicardipine on microglial cells: implications for neuroprotection. PloS one 2014;9:e91167.

[34] Choi W, Clemente N, Sun W, Du J, Lu W. The structures and gating mechanism of human calcium homeostasis modulator 2. Nature 2019;576:163-7.

[35] Syrjanen JL, Michalski K, Chou TH, Grant T, Rao S, Simorowski N, et al. Structure and assembly of calcium homeostasis modulator proteins. Nature structural & molecular biology 2020;27:150-9.

[36] Ma J, Qi X, Yang C, Pan R, Wang S, Wu J, et al. Calhm2 governs astrocytic ATP releasing in the development of depression-like behaviors. Mol Psychiatry 2018;23:883-91.

[37] Ferrer-Acosta Y, Rodriguez Cruz EN, Vaquer Adel C, Vega IE. Functional and structural analysis of the conserved EFhd2 protein. Protein and peptide letters 2013;20:573-83.

[38] Yin L, Dai Q, Jiang P, Zhu L, Dai H, Yao Z, et al. Manganese exposure facilitates microglial JAK2-STAT3 signaling and consequent secretion of TNF-a and IL-1beta to promote neuronal death. Neurotoxicology 2018;64:195-203.